Combined use of bacteriophage K and a novel bacteriophage to reduce *Staphylococcus aureus* biofilm

Alves, D.R.[1] Gaudion, A.[1], Bean, J.E.[1], Perez-Esteban, P.[2], Arnot T.[2], Harper, D.R.[3], Kot W.[4], Hansen, L.H.[4,5], Enright, M.C.[1a], A. Tobias A. Jenkins[1, a, b]

[1]*Department of Chemistry, University of Bath, Claverton Down, Bath, BA2 7AY, UK.*

[2]*Department of Chemical Engineering, University of Bath, Claverton Down, Bath, BA2 7AY, UK.*

[3]*AmpliPhi Biosciences Corp., Colworth Science Park, Sharnbrook, Bedfordshire, MK44 1LQ, UK*

[4]*Section of Microbiology, Department of Biology, University of Copenhagen, 2100 Copenhagen, Denmark*

[5]*Department of Environmental Science, Aarhus Universitet, Frederiksborgvej 399, Postboks, 358, DK-4000 Roskilde, Denmark*

[a] These authors contributed equally to this work

[b]Corresponding author – A. T. A. Jenkins (a.t.a.jenkins@bath.ac.uk)

Tel: +44 1225 386118

Email: a.t.a.jenkins@bath.ac.uk

Conflict of interest statement:

The authors declare that they have no conflicts of interest.

ABSTRACT

Biofilms are major causes of impairment of wound healing and patient morbidity. One of the most common and aggressive wound pathogens is *Staphylococcus aureus*, displaying a a large repertoire of virulence factors and commonly reduced susceptibility to antibiotics, such as the spread of methicillin-resistant *S. aureus* (MRSA). Bacteriophages are obligate parasites of bacteria. They multiply intracellularly and lyse their bacterial host releasing their progeny. We isolated a novel phage, DRA88 that has a broad host range amongst *S. aureus*. Morphologically the phage belongs to the *Myoviridae* family and comprises a large dsDNA genome of 141,907 bp. DRA88 was mixed with phage K to produce a high titre mixture that showed strong lytic activity against a wide range of *S. aureus* isolates including representatives of the major international MRSA clones and coagulase-negative *Staphylococcus*. Its efficacy was assessed both in planktonic cultures and when treating established biofilms produced by three different biofilm producing *S. aureus* isolates. A significant reduction of biofilm biomass over 48 hours of treatment was recorded in all cases. The phage mixture may form the basis of an effective treatment for infectious caused by *S. aureus* biofilms.

Key words: *Staphylococcus aureus*, bacteriophage therapy, biofilm, antibiotic resistant bacteria, MRSA, sequence analysis.

INTRODUCTION

Staphylococcus aureus is an opportunistic human bacterial pathogen that primarily colonizes the anterior nares (1) but is frequently shed onto skin surfaces. When an opportunity occurs that facilitates its penetration of the skin surface, it is able to cause a broad spectrum of human diseases, from skin and soft-tissue infections to systemic infections such as pneumonia, meningitis and osteomyelitis (1, 2). Host invasion and immune evasion is possible due to a myriad of virulence factors, including toxins, adhesins and evasins (3). In addition, *S. aureus* infections often comprise strains with antibiotic resistance. Examples of these are penicillin and methicillin resistant *S. aureus* (MRSA) and isolates with decreased susceptibility to vancomycin (4).

S. aureus is one of the most common gram-positive causes of wound infectious (5, 6). The wound environment is an ideal one for establishment of a bacterial infection as it contains large aggregations of necrotic tissue and accumulations of protein exudate (7). It is also observed that wound infections are strongly associated with the formation of biofilm communities (8). Once in a biofilm, bacterial cells experience greater protection against antibiotics and against elements of the host immune system, when compared to cells growing in a planktonic state (9). For example, the exopolysaccharide matrix blocks antibody penetration into biofilm (10) and phagocytes are unable to interact with bacterial cells (11). Biofilm structures are believed to be present in many acute wounds, but are very common in chronic wounds (12), and are a major factor delaying wound healing (12, 13). Moreover, many biofilms colonize implanted medical devices (14) greatly increasing patient morbidity and mortality and they are associated with larger health care costs (15). Chronic wounds affect 6.5 million patients in the United States and more than US$25 billion are spent every year on treatment (16).

Current antibiotic options to successfully treat *S. aureus* are becoming scarce despite the development of some novel drugs (17), and there is a growing need for effective agents to combat infections (18). Bacteriophage therapy is a viable alternative / adjunct to antibiotics in treating bacterial infection (for review see (19)). Bacteriophages (phages) are viruses able to infect highly specifically and kill the bacterial species targeted, but not eukaryotic cells. The phage-encoded lysis proteins – endolysin and holin - cause the breakdown of the bacterial membrane (20) resulting in cell death and release of phage particles.

Several studies have shown the potential of using phages to treat *S. aureus* infections (21–23) and it has been demonstrated that phages also have the ability to disrupt bacterial biofilms (24). Phages are increasingly recognized as serious candidates in the fight against antibiotic resistant bacteria in human therapeutics and as prophylaxis (25). Phages with strictly lytic life cycles, which result in a rapid killing of the target host and diminish the chances for bacteria to evolve towards phage resistance, are preferred for bacteriophage therapy use (26). It is also of value for the phage (or phage mixture) used to have a polyvalent nature, i.e. is able to infect a large set of strains within a species and may show improved applicability in situations where the etiological agent of an infectious disease has not been identified.

Here we investigate the potential of using two lytic and polyvalent *S. aureus* phages: K, a well-documented staphylococcal phage (27–29) that attaches specifically to the cell wall teichoic acid (30) providing a wide host range; and a newly isolated phage, DRA88. Phage K was, previously, shown to be able to disrupt biofilms produced by *S. aureus* strains (28). Here, we characterized the antimicrobial activity of the phages alone and in combination in planktonic and biofilm systems.

MATERIALS AND METHODS

Bacteria and Growth Conditions

S. aureus strains (listed in Table 1) used in this study were from our collection of >5000 clinical isolates and they were selected to be genetically diverse (by multilocus sequence typing (31)) and also to contain members of the major MRSA and MSSA clones present worldwide. Examples of eight coagulase-negative staphylococci: *S. xylosus*, *S. sciuri* subsp. *sciuri*, *S. chromogenes*, *S. hyicus*, *S. arlettae*, *S. vitulinus*, *S. simulans* and *S. epidermidis* were also included in this study. Bacteria from 5% (v/v) blood agar plates were grown at 37 ºC with constant shaking (170 rpm) in Tryptic Soy Broth (TSB). Tryptic Soy Agar (TSA) and TSB-soft-agar containing 0.65% of bacteriological agar were used for bacteriophage propagation and plaque count assays. Note that media was supplemented with 1mM $CaCl_2$ and $MgSO_4$ to improve phage adsorption (32). Bacterial aliquots were stocked at -80°C in broth containing 15% glycerol (v/v).

Bacteriophage Isolation

Bacteriophages were isolated from crude sewage (Thames Water PLC, Luton, UK). Bacterial enrichments with *S. aureus* isolates were performed to increase phage numbers as follows: 5 ml of actively growing *S. aureus* cells (from overnight liquid culture in TSB) and TSB supplemented with 1 mM $MgSO_4$ and 1 mM $CaCl_2$. The enrichment was incubated overnight at 37 ºC. A 10 ml aliquot was taken from the overnight culture and 1 M NaCl and 0.2% chloroform were added. The culture was then centrifuged (30 min, 3000 x g) to remove bacteria and the supernatant was filtered sterilized (0.22 µm pore size, Millipore filter). This lysate (supernatant) was used to check the presence of lytic phages using the double layer method as described previously (33). Isolated single plaques were picked into SM buffer (5 M NaCl, 1M MgSO4, 1 M Tris–HCl [pH 7.5], gelatine solution

distilled water) and successive rounds of single plaque purification were carried out until purified plaques were obtained, reflected by single plaque morphology. Purified phages were stored in 50% glycerol (v/v) at -80 ºC for long term use. Short term stock preparations were maintained at 4 ºC.

Bacteriophage Propagation

Phage lysates were propagated on their respective bacterial hosts. Briefly, 100 µl of phage lysate and 100 µl of host growing culture were mixed and left for 5 min at room temperature. Afterwards 3 ml of soft-agar was added and poured onto TSA plates. The following day, after an overnight incubation at 37 ºC, plates displaying confluent lysis were selected and 3 ml of SM buffer and 2% chloroform were added before incubating at 37 ºC for 4 h. High titre phage solution was removed from the plates, and centrifuged (8,000 x g, 10 min) to remove cell debris, then filter sterilized (pore size, 0.22 µm) and stored at 4 ºC. Both phages were propagated in the prophage-free isolate *S. aureus* RN4220 (40) to avoid potential contamination with mobilized phages (34).

Sensitivity Assay

To determine phage sensitivity of bacterial isolates spot tests were performed. Briefly, 3 ml of TSB-soft-agar was added to 100 µl of host growing culture and poured onto TSA. Plates were left to dry for 20 min at 37 ºC. The different phage lysates were standardized to a titre of 10^9 PFU/ml and 10 µl of each lysate were spotted onto the bacterial lawns. This assay was performed in triplicate. The plates were allowed to dry before incubating overnight at 37 ºC. The following day the sensitivity profiles of each of the bacterial strains were determined: if the bacterial lawn was lysed; slightly disrupted; or not disrupted, the bacterial isolate was labelled: sensitive; intermediate; or resistant to the phage infection.

Bacteriophage adsorption

The experiment was carried out at 37 ºC under constant shaking (60 rpm) and a phage inoculum of MOI (Multiplicity Of Infection) = 0.01. The number of free phages was calculated from the PFU of chloroform-treated samples within 5 min after inoculation. The adsorption rate, assuming a first order kinetics was calculated in terms of the percentage of free phage loss by fitting phage decay curve (normalized as a percentage) to the rate equation:

$$\ln(\%\ \text{phage})_t = \ln(\%\ \text{phage})_o - k't \qquad (1)$$

Where k' is the pseudo 1st rate constant for free phage loss:

$$k' = k[\text{bacteria}] \qquad (2)$$

From this, the percentage phage remaining at any time t can be easily calculated.

One-step growth curve

Phage growth cycle parameters - the latent period (L), eclipse period (E) and burst size (B), were determined from the dynamical change of the number of free and total phages. Hence, one-step growth curves were measured as described by Pajunen *et al.* (35) with some modifications: 10 ml of a mid-exponential-phase culture were harvested by centrifugation (7,000x g, 10 min, 4ºC) and resuspended in 5 ml TSB to obtain OD_{600} of 1.0. To this suspension, 5 ml of phage solution were added to obtain a MOI (multiplicity of infection) of 0.001. Phages were allowed to adsorb for 5 min at room temperature. The mixture was than centrifuged as described above and the pellet was resuspended in 10 ml of

172 fresh TSB medium. Two samples were taken every 5 min over a period of 1 h at 37 ºC
173 under constant shaking. The first samples were plated immediately without any treatment
174 and the second set of samples was plated after treatment with 1 % (v/v) chloroform to release
175 intracellular phages.
176
177 **Measurement of phage zeta potential and size**
178 The particle size and electrophoretic mobility of the phages was measured by Dynamic
179 Light Scattering (DLS) using a Zetasizer Z/S (Malvern, UK) at 37 °C. Cuvettes filled with
180 the sample were carefully inspected to avoid air bubbles. Phages were diluted in dH_2O to a
181 final concentration of 10^8 PFU ml^{-1}. Measurements were repeated at least three times.
182
183 **Electron Microscopy**
184 Phage particles in water were deposited on carbon coated copper grids and negatively stained
185 with 1% uranyl acetate (pH 4). Visualization was performed using a transmission electron
186 microscope (TEM) (JEOL JEM1200EXII, Bath, UK) operated at 120 kV.
187
188 **Phage DNA Extraction**
189 Concentrated phage preparations were obtained by a caesium chloride (CsCl) (Sigma,
190 UK) gradient composed of three different solutions with densities of: 1.35, 1.50 and 1.7 g
191 ml^{-1}. They were prepared in a 36.5 ml ultracentrifuge tube (Beckman Coulter, Seton
192 Scientific, UK). For the preparation of CsCl solution at a given density, ρ (g ml^{-1}), the
193 following equation was used to calculate the final CsCl concentration, c (g ml^{-1}): $c = 0.0478\rho^2 + 1.23\rho - 1.27$ as well as the protocol described previously by Boulanger (36).
194
195 After ultracentrifugation for 3 hours (75,600 g at 4 ºC) the phage band was collected and

196 dialysis was performed to remove CsCl residuals. Briefly, phage suspension was washed
197 into dialysis cassettes (Slide-A-Lyser, Fisher, UK), which in turn were introduced in 500
198 volumes of dialysis buffer (10 mM sodium phosphate, pH 7) for 30 min. After performing
199 the process three times the concentrated and purified phage suspension was collected.
200 Phenol/chloroform extraction was performed according to (37). 1.8 ml of phage lysates were
201 treated with 18µl DNase I (1 mg ml^{-1}) (Sigma Aldrich) and 8 µl RNase A (10 mg ml^{-1})
202 (Sigma Aldrich) and incubated at 37 ºC for 60 min. Subsequently, 18 µl proteinase K (10
203 mg ml^{-1}) (Sigma Aldrich), 1% of sodium dodecyl sulphate (SDS) and 1 mM EDTA.Na_2
204 were added to the samples and these were incubated at 65 ºC for further 60 min. All
205 protein material was eliminated by using phenol:chloroform:isoamyl alcohol (25:24:1)
206 (Sigma Aldrich) and DNA extraction and precipitation was performed as described
207 previously elsewhere (38). Nucleic acid concentration and quality was assessed with a
208 Nanodrop spectrophotometer (Thermo Scientific, UK).
209
210 **DNA sequencing, analysis and assembly**
211 DNA sequencing libraries were prepared using the Nextera® XT DNA kit (Illumina, San
212 Diego, USA) according to the manufacturer's protocol. Individually tagged libraries were
213 sequenced as a part of a flowcell as 2x250 base paired-end reads using the Illumina MiSeq
214 platform (Illumina, San Diego, USA) at The Danish National High-Throughput DNA-
215 Sequencing Centre. Reads were analysed, trimmed and assembled using 6.5.1 CLC
216 Genomic Workbench as described before by Kot *et al.* (39). Genes were predicted and
217 annotated using RAST server (40).
218 **Planktonic cultures treated with phage mixture**
219 Planktonic cultures were performed in 96-well microtitre plates and their optical density
220 was measured. In summary, a 1:100 dilution was prepared in the wells of the microplate by

adding 2 µl of an overnight culture to 198 µl of TSB. After 2 hours of incubation at 37 ºC, the single or mixed phage at a MOI of 0.1 was added and the microplates were incubated for a further 24 hours. The incubation was followed on a plate reader (FLUOstar Omega, BMG LabTech, UK) where the growth curves were established at an optical density at 590 nm (OD_{590}). This approach allows observation of the phage-bacteria interaction over time and also allows for monitoring of the appearance of resistant mutants for each phage lysate.

Biofilm formation

Biofilm assay was performed similarly to previously described methods (41), but with some modifications in order to optimize the system. Biofilm formation was performed in 96-well polystyrene tissue culture microplates (Nunclon™ Delta Surface, Nunc, UK) to achieve an improved cell attachment. TSB supplemented with 1% D-(+)-glucose (TSBg) and 1% NaCl (TSBg+NaCl) was used to perform this assay as this helps to improve biofilm formation (37, 38). An overnight culture was diluted to a titre of 10^8 cfu ml^{-1}. Briefly, in the microplate wells a 1:100 dilution was performed by adding 2 µl of the bacterial suspension to 198 µl of TSBg+NaCl, making a starting inoculum of 10^6 cfu ml^{-1}. 200 µl of broth were added to a set of wells as a negative control. All wells were replicated three times. Afterwards, microplates were incubated at 37 ºC for 48 hours with no shaking for biofilm formation. During the incubation time (~24 hours after incubation), 50 µl of fresh TSBg + NaCl was added to all control and test wells. Following incubation, medium was poured off and wells were carefully washed twice with sterile phosphate buffered saline (PBS) solution (Sigma Aldrich, UK) to remove any planktonic cells. Microplates were allowed to dry for 1 hour at 50 ºC. To determine total biofilm biomass microplate wells were stained with 0.1% Crystal Violet (CV). After staining the wells were washed twice

with PBS solution and dried. Biofilm formation was determined by visual comparison of the stained wells and photographed.

Biofilm treatment with phage mixture

Biofilm formation was carried out as described above. Once biofilms were established and washed once with PBS, 100 µl of phage mixture in PBS was added to a set of wells. Two different MOIs were set up for the single or mixed phage: 1 and 10. 100 µl of PBS were added both to the isolate positive and negative controls. All the experiments were performed three times. After static incubation at 37 ºC microplates were washed and stained, as described before, at pre-determined time-points. To perform optical density readings of the staining intensity, 100 µl of 95% ethanol (v/v) was added to each well and optical density at 590 nm (OD590) was taken using a plate reader.

Data analysis

Comparisons between the different time points and the positive controls were made by performing a *Student's t-test* and a *p-value* < 0.05 was considered statistically significant for all cases. All tests were performed with a confidence level of 95%. Spread of data at the 95% confidence interval (CI) was estimated using the Winpepi freeware statistical analysis program (42).

Nucleotide sequence accession number

The genome sequence of phage DRA88 has been deposited in the GenBank database under accession number KJ888149.

RESULTS

Isolation and host range determination

Several lytic phages were isolated in crude sewage samples from a water treatment facility and tested against the *S. aureus* bacterial collection listed in Table 1 in order to isolate phages with broad host ranges. One phage, DRA88, presented a host infectivity coverage of 60.0% (95% CI: 50% - 69%; 57 isolates out of 95 were susceptible) and so was selected for further studies. Phage K was also tested and showed host coverage of 64.2% (95% CI: 54% - 73%; 61 isolates out of 95 were susceptible). These two phages were mixed in a phage mixture giving a total coverage of 73.7% (95% CI: 64% - 82%) of the *S. aureus* isolates assigned to 14 different MLST (Multilocus Sequence Typing) types. Infectivity of both phages was also tested on a group of coagulase-negative isolates, where DRA88 did not kill efficiently any of the isolates. Phage K showed also a weakly infectivity, however two of the isolates (*S. simulans* and *S. hyicus*) were sensitive (Table. 2).

Phage Growth Characteristics

The life cycle and adsorption affinity of phage DRA88 and phage K were assessed when growing in RN4220 *S. aureus* host at 37 °C. Firstly, one-step growth studies were performed to identify the different phases of a phage infection process. After infection, phage growth cycle parameters (L - latent, E - eclipse, and B – burst size) were determined (Fig. 1). In the system established, the eclipse and latent periods of DRA88 were, 15 min and 25 min, respectively. DRA88 yielded a burst size of 76PFU and phage K of 125 PFU per infected cell after 60 min. These phage life cycle values are in conformity with the values normally observed for T7 group phages (43). The adsorption efficiency of phages to the host was estimated with cells in the early logarithmic growth phase (Fig. 2). The adsorption rate (adsorption affinity) of the phages, when infecting actively growing *S.*

296 *aureus* RN4220, was measured. From equation (1), the rate constant for the adsorption (loss
297 of free phage) for phage K and DRA88 were calculated (Fig. 2), k' = 0.352 min-1 and k' =
298 0.252 min-1, respectively. Hence, although similar, after 5 minutes, 80.3% of phage K was
299 adsorbed to the bacteria and 71.6% of DRA88. After 10 min, values for free viral particles
300 were below 5% for both phages.
301
302 **Morphology of phage particles**
303 The isolated phage DRA88 was further characterized with regard to its morphology.
304 Images of the phage DRA88 were developed using Transmission Electron Microscopy
305 (TEM). The results revealed that phage DRA88 has, along with an icosahedral head of ~ 78
306 nm in diameter, a long contractile tail of ~179 nm with tail fibers (Fig. 3A). Therefore it
307 can be classified as belonging to the *Myoviridae* family (order *Caudoviridales*),
308 according to the classification system of Ackermann (44). It was observed for phage
309 DRA88 that besides single phage particles there were also various aggregates made
310 through contact of their tail fibers (Fig. 3B). Phage K was also observed under TEM (Fig.
311 S1), revealing a viral particle also belonging to the *Myoviridae* family (27). The zeta
312 potential of phage DRA88 and phage K calculated from the electrophoretic mobility was
313 -17 mV and -26.3 mV, respectively. The size measured was 122 nm for phage K, but
314 according to the TEM micrographs and the literature this phage has an average size of 280
315 nm total (45). This discrepancy could be due to contraction of tails, which was observed
316 frequently, and can interfere with the measurement. Note that Dynamic Light Scattering
317 (DLS) may show lower accuracy when measuring irregular shaped particles, such as tailed
318 phages, where the size is not uniform in all dimensions. Regarding phage DRA88 we were
319 not able to obtain an accurate size measurement and this can be related to the phenomena of
320 aggregation observed under TEM.

Genomic characterization of DRA88 and comparison with phage K

To gain a more ample understanding of the phage DRA88, its DNA was extracted and genome sequencing performed. Upon assembly and annotation it was found that phage DRA88 has a large double stranded DNA genome with terminal redundancy, which suggests that phage DRA88 has a headful packaging system (46). The genome comprises 141,907 bp and can be grouped into the class III of Staphylococcal phages (>125kbp) (47); 204 putative coding regions and four tRNA genes were identified (Fig. 5 and Table 1 in Supplementary Data). The gene coding potential with 1.44 genes per kb, exhibits a high gene density. The majority of genes, 145 (71%), are found in the forward strand and 59 (29%) in the opposite strand. tRNA genes are all located in the reverse strand of the genome. Regarding the GC% content it shows 30.4%, a lower percentage than the one found in the *S. aureus* host – 32.9%. The amino acid sequence was found to share strong similarities (>95%) with several other phages, such as JD007 and GH15 previously sequenced (48, 49). A comparison between phage DRA88 and phage K was performed using the BLAST algorithm (48). DRA88 genome seems to be organized into functional modules – cell lysis, DNA replication and structural elements – highly similar to the organization of phage K and other staphylococcal *Myoviridae* phages belonging to the Twort-like viruses (47, 50, 51). Between these modules we can find several putative coding regions that are not yet found in the NCBI database or have no attributed function (phage and hypothetical proteins). These unknown functions represent 84.81% of the coding capacity. Three potential coding regions (orf178, orf192 and orf195) did not have any identical match with phage genes in the NCBI database. DRA88 lysin and DNA polymerase are not interrupted by introns (49), contrary to phage K, but similarly to phage GH15. At the end of the genome (between orf164 and orf182) there is a large coding region with unidentified functions inserted into the DRA88 genome that is not

observed in phage K. Also, DRA88 genome analysis did not reveal similarity to known virulent associated or toxin proteins.

Bacteriophage mixture inhibits planktonic bacterial growth

The efficacy of single DRA88 and phage K and their combination was assessed when treating bacterial cultures. Single phages and the phage mixture (MOI = 0.1) were introduced in a bacterial culture already growing for two hours under planktonic conditions and let to incubate for further 22 hours (Fig. 5). Single phage treatment showed to be less successful in general than the phage mixture and this was cleared observed for S. aureus 15981 isolate (Fig 5A). For all three *S. aureus* bacterial cultures – 15981, MRSA252 and H325 – no cell growth was observed when the phage mixture was present compared to bacterial growth only. In fact, we observed efficient inhibition of the bacterial growth for 15981 and H325. The same was not observed for MRSA 252, where we observed bacterial growth after 18 hours of treatment (time = 20 hours).

Biofilm eradication

Biofilms produced by the three *S. aureus* isolates were established in microtitre plates. All isolates were strong biofilm producers, however MRSA 252 followed by H325 isolates produced lower biofilm biomass and more fragile structure (when performing the mechanical washing steps the biofilm was more susceptible to disruption). The established biofilms were treated with single and mixed phage at MOI 10 and the biofilm was assessed (Figs 6 and 7). Measurement of biofilm density made using crystal violet / OD590 nm over 48 hours showed a clear reduction following phage inoculation compared with non-treated controls ($p = < 0.05$). A decrease in biofilm biomass from the mixture compared with the single phages after 48 hours of treatment was seen in all cases, although not

significant it can been observed by eye (along with CV stained wells). Established biofilms were also treated with the phage mix at two different MOIs: 1 and 10, and the biofilm was assessed at the time points: 0h, 2h, 4h, 24h and 48h (Fig 8). Unsurprisingly, phage mixtures with higher MOIs (10 compared with 1) gave a more rapid reduction in biofilm density, although both MOIs of 1 and 10 resulted in the same endpoint after 48 hours. For *S. aureus* 15981 biofilms treated with MOI 10, 4 hours after treatment, there was already more than 50% biofilm reduction (*p-value* < 0.05) and after 48 hours of treatment the biofilm biomass was almost completely disrupted (MOI 10, *p-value* = 4.82×10^{-3}; MOI 1, *p-value* = 1.47×10^{-5}) (Fig. 8A). Figure 8B shows that biofilms produced by MRSA 252 were eliminated by more than 50% (MOI 10, *p-value* = 0.003; MOI 1, *p-value* = 0.012) after 48 hours of phage treatment. At last, biofilms produced by H325 were not initially as strong as the other isolates. However we were able to observe a reduction of the biofilms as well over 48 hours for MOI 10 (*p-value* = 0.049). For MOI 1 a reduction of the biofilm structure was observed after 24 hours (*p-value* = 0.034). However such reduction was not observed after 48 hours.

DISCUSSION

S. aureus biofilms in wounds and catheter sites present particular problems to patients , increasing morbidity, mortality and difficulty in delivering effective chemotherapy. For wound healing to occur, treatment of the biofilm infection is essential and often requires selection of the correct antibiotic. The choice of appropriate chemotherapy is however made more difficult due to the increasing prevalence of antibiotic resistance. Hence, solutions are required to avoid treatment delay or ineffectiveness.

The host range infectivity of DRA88 against a genetically diverse collection of *S. aureus* isolates was broad, showing that this is a polyvalent phage. Based on TEM analysis DRA88 belongs to the *Myoviridae* tailed- phage family. DRA88 adsorption occurred rapidly and at a similar rate to that observed for phage K, which is in accordance to several *S. aureus Myoviridae* infecting phages (52, 53). An interesting observation for phage DRA88 was the possible formation of phage aggregates. Phage aggregation is observed occasionally in nature (54, 55) and is dependent on pH, ionic strength and the composition of ions. Such phenomena could have been influenced by uranyl acetate (pH 4) used to stain the phages for TEM observation. However, DLS measurements (in d.H_2O: ~pH 7) were unsuccessful and possibly due to several sizes found in the sample (singles and several aggregates), hence, we suspect that phage DRA88 is prone to form aggregates. When interacting with bacterial cells, aggregation could impede phage access to the cells and hence slow the rate of adsorption. Phage aggregation can be inhibited by optimization of growth media composition or stabilised in nano-emulsions resulting in phages that more efficiently attach to bacterial cells (56–58), consequently this could affect estimation of the PFU which then may not directly correspond with the number of infective particles (MOI).

At the genome level, DRA88 was revealed to be a large dsDNA phage, usually a common characteristic of *Myoviridae* virus (50), carrying a high gene density and low GC%. It exhibits a high degree of relatedness to several other phages of the Twort-like group, including phage K. No virulence factors in the genome were identified, according to data available, suggesting that this phage could be safely used to treat *S. aureus* infections. The majority of putative coding regions of DRA88 genome do not have yet any function attributed yet, which is generally observed for the numerous phages being sequenced at the current time (59). Consequently, there is a crucial need for a more comprehensive investigation of phage genomes. Considering phage therapy as a therapeutic approach option, it is extremely important that we expand our knowledge regarding phage genes and proteins, and their respective functions and potentialities, as they can be involved in phage-host interaction and even code for novel virulence determinants (60).

The novel isolated phage was mixed into a phage mixture with phage K and as a result their lytic potential was increased (74 % of host coverage). The use of a phage mixture is largely preferred over use of single phage as it results in a decreased rate of bacteria exhibiting resistance (61, 62). Bacterial broth cultures growing with phage mixtures showed an elimination of bacterial cells and suppression of resistant mutants. However, this was only observed for two strains; after 18 hours of growth, MRSA 252 was able to counteract the infectivity of the phage particles present in the culture, possibly due to the presence of phage receptor mutated clones present in the culture. This situation could be overcome or delayed by including more phage types to the therapeutic mixture, a task far easier (more rapid and likely to succeed) to undertake compared to the discovery of a new antibiotic. It has been demonstrated that phage therapy could be delivered in synchronization with another antibacterial therapy, such as antibiotics (63). Reducing the initial bacterial load could be

445 sufficient to bring the bacterial numbers under control so that the drug and also the action of
446 the immune system can clear the infection (63–65) in an effective way.
447
448 More than 60% of all infections are related to the formation of biofilms (12). Hence, it is
449 important that biofilm model studies are investigated when testing a new antibacterial phage
450 mixture. Some studies already suggest the significant potential of phages to reduce and/or
451 eliminate biofilms. This is the case of phage K, where biofilms produced by *S. aureus* isolates
452 showed a remarkable decrease in their biofilm biomass after addition of the phage (28, 41).
453 Here, we showed that the phage mixture was able to reduce significantly the biofilm load on
454 the polystyrene surface a microtitre plate. For isolate 15981 the eradication effect started
455 readily after addition of the killing mixture and after 48 hours of treatment the biofilm was
456 almost completely disrupted. Higher MOI showed a more rapid effect of biofilm reduction and
457 a better prevention of biofilm regrowth was also observed for isolate H325. Comparing the
458 effect of phage mixture on broth cultures to biofilm we observed a more positive effect on
459 eliminating the bacterial load of broth cultures than that on biofilm, which is disrupted more
460 slowly. This scenario was hypothesized to be due the metabolic state of the cells. In biofilms,
461 cells can be in a low metabolic activity stage and phages cannot proliferate as efficiently as in
462 active growing cells (41). To date, very few studies have been performed regarding phage
463 mixture treatments, especially to treat *S. aureus* biofilms and in particular MRSA-caused ones.
464 Kelly *et al* (28) have already shown the efficacy of a phage K and derivatives mixture
465 on the eradication of *S. aureus* biofilms produced by non-human clinical isolates. Here we go
466 further by treating biofilms produced by prevalent human clinical isolates that also include
467 MRSA types. This study suggests that the utilisation of a mixture of bacteriophage i.e. phage
468 K and DRA88 in this case, could provide a practical alternative to antibiotic / antimicrobial
469 treatments for combating some *S. aureus* infections and in particular the devastating effects of

MRSA infections and biofilms related, such as burn-wound or catheter infection. Even with the contribution of this study on the effectiveness of bacteriophage therapy to fight established bacterial infections, there is still a long way to go and several barriers to address. The safety of phages and ethical and regulatory issues, for example, must be overcome in order to phages become an available alternative therapeutic (see review (66)).

In summary, here we describe the isolation and characterization of a novel bacteriophage against pathogenic *S. aureus* bacteria. The phage, in combination with phage K, showed an improved range of infectivity of *S. aureus* isolates and a potent effect in biofilm dispersion making it a good candidate for further therapeutic development.

ACKNOWLEDGEMENTS

The authors thank Thames Water for providing the water samples and Ursula Potter for her help with TEM analysis and sample preparation. The authors also thank AmpliPhi Biosciences Corp for their important collaboration and technical assistance and the Engineering and Physical Sciences Research Council (EPSRC) Healthcare Partnership fund for their funding and support. This work was partly supported by the MetaPhageLAB project financed by The Danish Research Council for Technology and Production (Project: 11-106991, Doc#: 2105568).

REFERENCES

1. **Lowy FD**. 1998. Staphylococcus aureus infections. N. Engl. J. Med. **339**:520–532.

2. **Foster TJ**. 2005. Immune evasion by staphylococci. Nat. Rev. Microbiol. **3**:948–958.

3. **Plata K, Rosato AE, Wegrzyn G**. 2009. Staphylococcus aureus as an infectious agent: overview of biochemistry and molecular genetics of its pathogenicity. Acta Biochim. Pol. **56**:597–612.

4. **Chang S, Sievert DM, Hageman JC, Boulton ML, Tenover FC, Downes FP, Shah S, Rudrik JT, Pupp GR, Brown WJ, Cardo D, Fridkin SK**. 2003. Infection with vancomycin-resistant Staphylococcus aureus containing the vanA resistance gene. N. Engl. J. Med. **348**:1342–7.

5. **Murray CK, Holmes RL, Ellis MW, Mende K, Wolf SE, McDougal LK, Guymon CH, Hospenthal DR**. 2009. Twenty-five year epidemiology of invasive methicillin-resistant Staphylococcus aureus (MRSA) isolates recovered at a burn center. Burns **35**:1112–7.

6. **Keen EF, Robinson BJ, Hospenthal DR, Aldous WK, Wolf SE, Chung KK, Murray CK**. 2010. Prevalence of multidrug-resistant organisms recovered at a military burn center. Burns **36**:819–25.

7. **Erol S, Altoparlak U, Akcay MN, Celebi F, Parlak M**. 2004. Changes of microbial flora and wound colonization in burned patients. Burns **30**:357–361.

8. **Percival SL, Hill KE, Williams DW, Hooper SJ, Thomas DW, Costerton JW**. 2012. A review of the scientific evidence for biofilms in wounds. Wound Repair Regen. **20**:647–57.

9. **Høiby N, Bjarnsholt T, Givskov M, Molin S, Ciofu O**. 2010. Antibiotic resistance of bacterial biofilms. Int. J. Antimicrob. Agents **35**:322–332.

10. **De Beer D, Stoodley P, Lewandowski Z**. 1997. Measurement of local diffusion coefficients in biofilms by microinjection and confocal microscopy. Biotechnol. Bioeng. **53**:151–8.

11. **Lam J, Chan R, Lam K, Costerton JW**. 1980. Production of mucoid microcolonies by Pseudomonas aeruginosa within infected lungs in cystic fibrosis. Infect. Immun. **28**:546–56.

12. **James GA, Swogger E, Wolcott R, Pulcini E deLancey, Secor P, Sestrich J, Costerton JW, Stewart PS**. 2008. Biofilms in chronic wounds. Wound Repair Regen. **16**:37–44.

13. **Davies CE, Hill KE, Wilson MJ, Stephens P, Hill CM, Harding KG, Thomas DW**. 2004. Use of 16S ribosomal DNA PCR and denaturing gradient gel electrophoresis for

analysis of the microfloras of healing and nonhealing chronic venous leg ulcers. J. Clin. Microbiol. **42**:3549–57.

14. **Donlan RM**. 2008. Biofilms on central venous catheters: is eradication possible? Curr. Top. Microbiol. Immunol. **322**:133–61.

15. **Darouiche RO**. 2004. Treatment of infections associated with surgical implants. N. Engl. J. Med. **350**:1422–9.

16. **Sen CK, Gordillo GM, Roy S, Kirsner R, Lambert L, Hunt TK, Gottrup F, Gurtner GC, Longaker MT**. 2010. Human skin wounds: a major and snowballing threat to public health and the economy. Wound Repair Regen. **17**:763–71.

17. **Liapikou A, Torres A**. 2013. Emerging drugs on methicillin-resistant Staphylococcus aureus. Expert Opin. Emerg. Drugs **18**:291–305.

18. **Kurlenda J, Grinholc M**. 2012. Alternative therapies in Staphylococcus aureus diseases. Acta Biochim. Pol. **59**:171–84.

19. **Burrowes B, Harper DR, Anderson J, McConville M, Enright MC**. 2011. Bacteriophage therapy: potential uses in the control of antibiotic-resistant pathogens. Expert Rev. Anti. Infect. Ther. **9**:775–785.

20. **Young I, Wang I, Roof WD**. 2000. Phages will out: strategies of host cell lysis. Trends Microbiol. **8**:120–8.

21. **Kraushaar B, Thanh MD, Hammerl JA, Reetz J, Fetsch A, Hertwig S**. 2013. Isolation and characterization of phages with lytic activity against methicillin-resistant Staphylococcus aureus strains belonging to clonal complex 398. Arch. Virol. **158**:2341–50.

22. **Capparelli R, Parlato M, Borriello G, Salvatore P, Iannelli D**. 2007. Experimental phage therapy against Staphylococcus aureus in mice. Antimicrob. Agents Chemother. **51**:2765–73.

23. **Gupta R, Prasad Y**. 2011. Efficacy of polyvalent bacteriophage P-27/HP to control multidrug resistant Staphylococcus aureus associated with human infections. Curr. Microbiol. **62**:255–60.

24. **Abedon ST**. 2011. Bacteriophages and Biofilms: Ecology, Phage Therapy, Plaques. Nova Science Publishers.

25. **Górski A, Miedzybrodzki R, Borysowski J, Weber-Dabrowska B, Lobocka M, Fortuna W, Letkiewicz S, Zimecki M, Filby G**. 2009. Bacteriophage therapy for the treatment of infections. Curr. Opin. Investig. Drugs **10**:766–74.

26. **Skurnik M, Pajunen M, Kiljunen S**. 2007. Biotechnological challenges of phage therapy. Biotechnol. Lett. **29**:995–1003.

27. **O'Flaherty S, Ross RP, Meaney W, Fitzgerald GF, Elbreki MF, Coffey A**. 2005. Potential of the polyvalent anti-Staphylococcus bacteriophage K for control of antibiotic-resistant staphylococci from hospitals. Appl. Environ. Microbiol. **71**:1836–1842.

28. **Kelly D, McAuliffe O, Ross RP, Coffey A**. 2012. Prevention of Staphylococcus aureus biofilm formation and reduction in established biofilm density using a combination of phage K and modified derivatives. Lett. Appl. Microbiol. **54**:286–91.

29. **O'Flaherty S, Coffey A, Edwards R, Meaney W, Fitzgerald GF, Ross RP**. 2004. Genome of staphylococcal phage K: a new lineage of Myoviridae infecting gram-positive bacteria with a low G+C content. J. Bacteriol. **186**:2862–71.

30. **Xia G, Corrigan RM, Winstel V, Goerke C, Gründling A, Peschel A**. 2011. Wall teichoic Acid-dependent adsorption of staphylococcal siphovirus and myovirus. J. Bacteriol. **193**:4006–9.

31. **Enright MC, Day NP, Davies CE, Peacock SJ, Spratt BG**. 2000. Multilocus sequence typing for characterization of methicillin-resistant and methicillin-susceptible clones of Staphylococcus aureus. J. Clin. Microbiol. **38**:1008–15.

32. **TUCKER RG**. 1961. The role of magnesium ions in the growth of Salmonella phage anti-R. J. Gen. Microbiol. **26**:313–23.

33. **Adams M**. 1959. Bacteriophages. Interscience Publishers Inc, New York.

34. **Nirmal Kumar GP, Sundarrajan S, Paul VD, Nandini S, Saravanan RS, Hariharan S, Sriram B, Padmanabhan S**. 2012. Use of prophage free host for achieving homogenous population of bacteriophages: new findings. Virus Res. **169**:182–7.

35. **Pajunen M, Kiljunen S, Skurnik M**. 2000. Bacteriophage phiYeO3-12, specific for Yersinia enterocolitica serotype O:3, is related to coliphages T3 and T7. J. Bacteriol. **182**:5114–20.

36. **Boulanger P**. 2009. Purification of bacteriophages and SDS-PAGE analysis of phage structural proteins from ghost particles. Methods Mol. Biol. **502**:227–238.

37. **Pickard DJJ**. 2009. Preparation of bacteriophage lysates and pure DNA. Methods Mol. Biol. **502**:3–9.

38. **Sambrook J, Russell DW**. 2001. Molecular Cloning - Sambrook & Russel - Vol. 1, 2, 3. CSH Press.

39. **Kot W, Vogensen FK, Sørensen SJ, Hansen LH**. 2014. DPS - A rapid method for genome sequencing of DNA-containing bacteriophages directly from a single plaque. J. Virol. Methods **196**:152–6.

40. **Aziz RK, Bartels D, Best AA, DeJongh M, Disz T, Edwards RA, Formsma K, Gerdes S, Glass EM, Kubal M, Meyer F, Olsen GJ, Olson R, Osterman AL,**

Overbeek RA, McNeil LK, Paarmann D, Paczian T, Parrello B, Pusch GD, Reich C, Stevens R, Vassieva O, Vonstein V, Wilke A, Zagnitko O. 2008. The RAST Server: rapid annotations using subsystems technology. BMC Genomics **9**:75.

41. **Cerca N, Oliveira R, Azeredo J**. 2007. Susceptibility of Staphylococcus epidermidis planktonic cells and biofilms to the lytic action of staphylococcus bacteriophage K. Lett. Appl. Microbiol. **45**:313–7.

42. **Abramson JH**. 2011. WINPEPI updated: computer programs for epidemiologists, and their teaching potential. Epidemiol. Perspect. Innov. **8**:1.

43. **Sillankorva S, Neubauer P, Azeredo J**. 2008. Isolation and characterization of a T7-like lytic phage for Pseudomonas fluorescens. BMC Biotechnol. **8**:80.

44. **Ackermann H**. 2011. Bacteriophage taxonomy. Microbiol. Aust. 90–94.

45. **Rees PJ, Fry BA**. 1981. The morphology of staphylococcal bacteriophage K and DNA metabolism in infected Staphylococcus aureus. J. Gen. Virol. **53**:293–307.

46. **Streisinger G, Emrich J, Stahl MM**. 1967. Chromosome structure in phage t4, iii. Terminal redundancy and length determination. Proc. Natl. Acad. Sci. U. S. A. **57**:292–5.

47. **Kwan T, Liu J, DuBow M, Gros P, Pelletier J**. 2005. The complete genomes and proteomes of 27 Staphylococcus aureus bacteriophages. Proc. Natl. Acad. Sci. U. S. A. **102**:5174–5179.

48. **Cui Z, Song Z, Wang Y, Zeng L, Shen W, Wang Z, Li Q, He P, Qin J, Guo X**. 2012. Complete genome sequence of wide-host-range Staphylococcus aureus phage JD007. J. Virol. **86**:13880–1.

49. **Gu J, Liu X, Lu R, Li Y, Song J, Lei L, Sun C, Feng X, Du C, Yu H, Yang Y, Han W**. 2012. Complete genome sequence of Staphylococcus aureus bacteriophage GH15. J. Virol. **86**:8914–5.

50. **Deghorain M, Van Melderen L**. 2012. The Staphylococci Phages Family: An Overview. Viruses **4**:3316–3335.

51. **Łobocka M, Hejnowicz MS, Dąbrowski K, Gozdek A, Kosakowski J, Witkowska M, Ulatowska MI, Weber-Dąbrowska B, Kwiatek M, Parasion S, Gawor J, Kosowska H, Głowacka A**. 2012. Genomics of staphylococcal Twort-like phages--potential therapeutics of the post-antibiotic era. Adv. Virus Res. **83**:143–216.

52. **Hsieh S-E, Lo H-H, Chen S-T, Lee M-C, Tseng Y-H**. 2011. Wide host range and strong lytic activity of Staphylococcus aureus lytic phage Stau2. Appl. Environ. Microbiol. **77**:756–61.

53. **Kwiatek M, Parasion S, Mizak L, Gryko R, Bartoszcze M, Kocik J**. 2012. Characterization of a bacteriophage, isolated from a cow with mastitis, that is lytic against Staphylococcus aureus strains. Arch. Virol. **157**:225–34.

638 54. **Hejkal TW, Wellings FM, Lewis AL, LaRock PA**. 1981. Distribution of viruses
639 associated with particles in waste water. Appl. Environ. Microbiol. **41**:628–34.

640 55. **Narang HK, Codd AA**. 1981. Frequency of preclumped virus in routine fecal
641 specimens from patients with acute nonbacterial gastroenteritis. J. Clin. Microbiol.
642 **13**:982–8.

643 56. **Langlet J, Gaboriaud F, Gantzer C**. 2007. Effects of pH on plaque forming unit
644 counts and aggregation of MS2 bacteriophage. J. Appl. Microbiol. **103**:1632–8.

645 57. **Zemb O, Manefield M, Thomas F, Jacquet S**. 2013. Phage adsorption to bacteria in
646 the light of the electrostatics: a case study using E. coli, T2 and flow cytometry. J.
647 Virol. Methods **189**:283–9.

648 58. **Esteban PP, Alves DR, Enright MC, Bean JE, Gaudion A, Jenkins ATA, Young**
649 **AER, Arnot TC**. 2014. Enhancement of the antimicrobial properties of bacteriophage-
650 K via stabilization using oil-in-water nano-emulsions. Biotechnol. Prog. **30**, 932-944.

651 59. **Hatfull GF**. 2008. Bacteriophage genomics. Curr. Opin. Microbiol. **11**:447–53.

652 60. **Lima-Mendez G, Toussaint A, Leplae R**. 2011. A modular view of the bacteriophage
653 genomic space: identification of host and lifestyle marker modules. Res. Microbiol.
654 **162**:737–46.

655 61. **Tanji Y, Shimada T, Fukudomi H, Miyanaga K, Nakai Y, Unno H**. 2005.
656 Therapeutic use of phage cocktail for controlling Escherichia coli O157:H7 in
657 gastrointestinal tract of mice. J. Biosci. Bioeng. **100**:280–287.

658 62. **Gu J, Liu X, Li Y, Han W, Lei L, Yang Y, Zhao H, Gao Y, Song J, Lu R, Sun C,**
659 **Feng X**. 2012. A method for generation phage cocktail with great therapeutic
660 potential. PLoS One **7**:e31698.

661 63. **Ryan EM, Alkawareek MY, Donnelly RF, Gilmore BF**. 2012. Synergistic phage-
662 antibiotic combinations for the control of Escherichia coli biofilms in vitro. FEMS
663 Immunol. Med. Microbiol. **65**:395–8.

664 64. **Comeau AM, Tétart F, Trojet SN, Prère M-F, Krisch HM**. 2007. Phage-Antibiotic
665 Synergy (PAS): beta-lactam and quinolone antibiotics stimulate virulent phage growth.
666 PLoS One **2**:e799.

667 65. **Kirby AE**. 2012. Synergistic action of gentamicin and bacteriophage in a continuous
668 culture population of Staphylococcus aureus. PLoS One **7**:e51017.

669 66. **Henein A**. 2013. What are the limitations on the wider therapeutic use of phage?
670 Bacteriophage **3**:e24872.

671

672

673 **TABLE LEGENDS**

674 **Table 1:** Sensitivity screening[†] of phage mixture against 95 *S. aureus* isolates.
675 Further information regarding the isolate sequence type (ST) and origin are supplied.
676 [†] Bacterial isolates were Susceptible – clear spot (S, light grey), Intermediate – turbid
677 spot (I, medium grey) or Resistant – no disturbance of bacterial lawn (R, dark grey) to
678 phage infection.

679 **Table 2:** Sensitivity screening of phage mixture against coagulase-negative staphylococci
680 isolates. [†] Bacterial isolates were Susceptible – clear spot (S, light grey), Intermediate –
681 turbid spot (I, medium grey) or Resistant – no disturbance of bacterial lawn (R, dark grey) to
682 phage infection.

683

684 **FIGURE LEGENDS**

685 **Figure 1:** Curve One-step growth of phage DRA88 (left) and phage K (right) in
686 RN4220 *S. aureus* at 37 °C. Shown are the PFU per infected cell in untreated
687 cultures (●) and in chloroform-treated cultures (○) at several time points over 60
688 minutes. The phage growth parameters are indicated in the figure and correspond to:
689 E - eclipse period; L - latent period and B - burst size. Each data point is the mean
690 of three independent experiments and error bars indicate the mean ± standard
691 deviation.

692 **Figure 2:** Percentage of free (A) DRA88 and (B) Phage K phages after infection
693 of actively growing RN4220 *S. aureus* at a MOI of 0.001 at several time points over
694 10 minutes. Rate constants for loss of phage are 0.352 min^{-1} for Phage K and 0.252
695 min^{-1} for DRA88. Each data point is the mean of three independent experiments and
696 error bars indicate the mean ± standard deviation.

697 **Figure 3:** Electron micrograph images of phage DRA88 negatively stained with

698 1% uranyl acetate, (A) showing the tail in a contracted position and (B)
699 formation on phage particles aggregates. Scale bar is indicated.

700 **Figure 4:** Comparative genomic analysis of phage DRA88 and phage K. Nucleotide
701 sequences were compared using the Artemis Comparison Tool (ACT). Predicted ORFs
702 are denoted by arrows, tRNAs are indicated (vertical blue dashed line) and genes encoding
703 proteins with at least 69% amino acid identity between the two genomes are indicated by
704 shaded regions.

705 **Figure 5:** Dynamic of bacteria with single and phage mixture in liquid cultures over 24
706 hours incubation at 37 °C. Absorbance readings at 590nm were taken in a microtitre plate
707 reader. *S. aureus* isolates: A – 15981; B – MRSA 252; C – H325 growing with only SM
708 buffer (○), with single DRA88 (▼), with single phage K (△) and with the phage mixture in
709 SM buffer (■) and also a negative control only SM buffer (●) are shown in the figure. Assays
710 were performed four times and OD590 was expressed as the mean ± standard deviation.

711 **Figure 6 :** Normalized biofilm biomass treated with single phage K, DRA88 and the phage
712 mixture after 48 hours at MOI 10 (OD590 reading after CV staining). *S. aureus* isolates: 1 –
713 15981; 2 – MRSA 252; 3 – H325. Mean values for the three strains treated with: phage K =
714 0.63 (SD±0.10), 0.30 (SD±0.16), 0.27 (SD±0.06); DRA88 = 0.11 (SD±0.04), 0.18
715 (SD±0.08), 0.29 (SD±0.03) phage mixture = 0.06 (SD±0.02), 0.15 (SD±0.02), 0.23
716 (SD±0.02). Assays were performed three times and the mean ± standard deviation is
717 indicated. Statistically significance of biofilm reduction was assessed by performing a
718 *Student's t-test*. *p-values* are indicated (* : <0.05).

719 **Figure 7:** Visualization of wells stained with 0.1% of crystal violet after 48 hours of phage
720 treatment at MOI 10. Shown are the biofilm wells treated with PBS, phage K, DRA88 and
721 phage mixture at 0h (A) and (B) 48 hours after. Experiments were performed in triplicate.

722 **Figure 8:** Normalized biofilm biomass treated with the phage mixture over 48 hours at two

different MOIs (OD590 reading after CV staining). *S. aureus* isolates: A – 15981; B – MRSA 252; C – H325. Assays were performed three times and the mean ± standard deviation is indicated. Statistically significance of biofilm reduction was assessed by performing a *Student's t-test*. *p-values* are indicated (* : <0.05).

748 **Table 1**: Sensitivity screening[†] of phage mixture against 95 *S. aureus* isolates. Further
749 information regarding the isolate sequence type (ST) and origin are supplied.

Isolates	ST	Country	Phage K	DRA88	Phage mixture
WBG8343	1	Australia	S	I	S
MSSA H476	1	England	S	S	S
HT2001749	1	USA	S	I	S
H148	3	UK	S	S	S
CDC980193-USA800	5	USA	S	S	S
Mu3	5	Japan	S	R	S
963Small	5	USA	S	S	S
97.1948.S.	5	Scotland	R	R	R
C56	6	UK	S	S	S
C2	7	UK	I	I	I
CDC201114-USA300	8	USA	S	S	S
15981	8	Spain	I	S	S
HT20030203	8	USA	I	S	S
HT20030206	8	USA	S	I	S
C125	8	UK	I	I	I
Fra97392	8	France	I	R	I
EMRSA6	8	UK	I	I	I
99st22111	8	-	S	S	S
H169	9	UK	S	S	S
D316	11	UK	I	I	I
D329	12	England	S	S	S
H117	12	UK	S	S	S
H402	13	UK	S	S	S
C154	14	UK	S	S	S
C357	15	UK	S	S	S
H291	18	UK	S	I	S
H42	20	UK	S	S	S
HO50960412	22	UK	I	S	S
H182	22	England	S	S	S
C720	22	England	R	S	S
C13	22	Eire	S	S	S
C49	23	UK	S	S	S
D279	25	UK	I	I	I
Not116	27	UK	S	S	S
H118	28	UK	S	I	S
SwedenAO17934/97	30	Sweden	S	I	S
Cuba4030	30	Cuba	I	I	I

C390	31	UK	S	S	S
H399	33	UK	S	S	S
C160	34	UK	I	I	I
Btn766	36	UK	S	S	S
MRSA 252	36	England	S	S	S
H325	36	UK	S	S	S
EMRSA16	36	UK	S	S	S
H137	38	UK	I	I	I
H137MRSA	38	UK	S	S	S
C253	40	UK	I	I	I
C427	42	UK	S	S	S
Fin76167	45	Finland	S	S	S
C316	49	UK	S	S	S
H417	50	UK	S	S	S
C3	51	UK	S	S	S
D49	53	UK	S	S	S
D98	54	UK	I	I	I
D318	57	UK	S	S	S
D535	59	UK	I	I	I
HT20050306	59	Australia	I	I	I
H40	60	UK	S	S	S
D473	69	UK	I	I	I
CDC201078-USA700	72	USA	I	I	I
HT20040991	80	Algeria	S	R	S
SwedN8890/99	80	Sweden	I	I	I
BK1563	88	USA	I	S	S
HT20020635	93	Australia	S	I	S
HT2001634	93	Australia	I	S	S
HT20020635	93	USA	I	S	S
Cuba4005	94	Cuba	S	S	S
D302	97	UK	S	S	S
Not38	101	UK	S	S	S
D472	109	UK	S	S	S
H560	121	UK	S	S	S
D139	145	UK	I	I	I
D22	182	UK	I	I	I
Can6428-011	188	Canada	S	S	S
D470	207	UK	I	I	I
98/10618	217	UK	S	S	S
CDC12	225	USA	S	S	S
Germany131/98	228	Germany	S	S	S
CDC16	231	USA	S	S	S

99.3759V	235	Scotland	S	I	S
SwedenON408/99	246	Sweden	I	I	I
KD121618	250	Switzerland	S	I	S
KD12943	257	UK	I	I	I
Not271	264	UK	I	I	I
Not380	266	UK	I	S	S
Not98-53	280	UK	I	S	I
CAN6820-0616	289	Canada	I	I	I
Fin62305	296	Finland	S	I	S
Not266	301	UK	S	S	S
Btn2164	312	UK	S	S	S
Btn2299	322	UK	I	I	S
Btn2289	322	UK	S	S	S
515/09	398		S	S	S
Not161	517	UK	S	I	S
Not290	529	UK	S	S	S

† Bacterial isolates were Susceptible – clear spot (S, light grey), Intermediate – turbid spot (I, medium grey) or Resistant – no disturbance of bacterial lawn (R, dark grey) to phage infection.

Table 2: Sensitivity screening of phage mixture against coagulase-negative staphylococci

765 isolates.

Species	Isolates	k	DRA88	Phage Cocktail
S. xylosus	ATCC 29971	I	I	I
S. sciuri subsp. *sciuri*	ATCC 29062	I	I	I
S. chromogenes	CCM 3387	I	I	I
S. hyicus	CCM 29368	S	I	S
S. arlettae	N910 254	I	I	I
S. vitulinus	ATCC 51145	I	I	I
S. simulans	N920 197	S	I	S
S. epidermidis	ATCC 14990	I	R	I

766 † Bacterial isolates were Susceptible – clear spot (S, light grey), Intermediate – turbid spot (I,
767 medium grey) or Resistant – no disturbance of bacterial lawn (R, dark grey) to phage
768 infection.

769

770

771

772

773

774

775

776

777

778

779

780

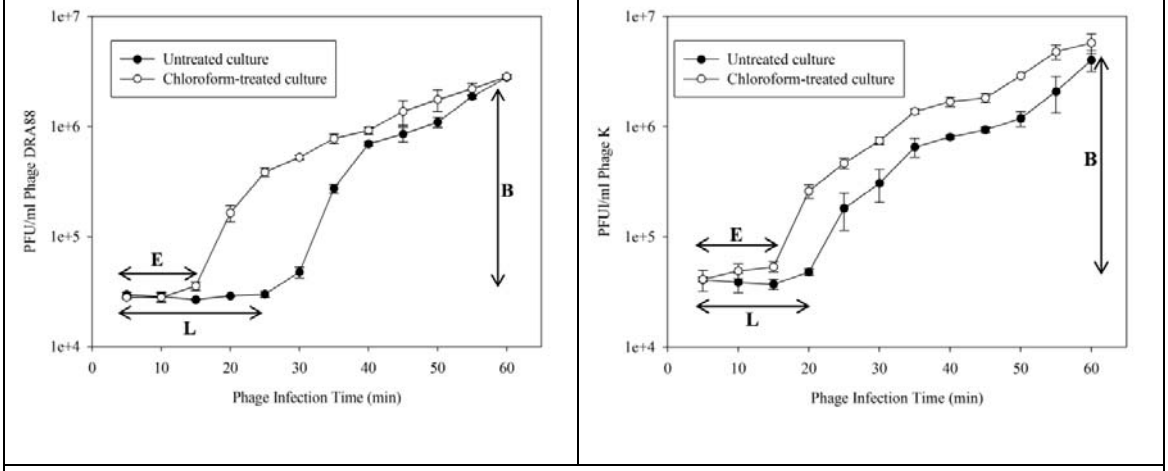

Figure 1: Curve One-step growth of phage DRA88 (left) and phage K (right) in RN4220 *S. aureus* at 37 °C. Shown are the PFU per infected cell in untreated cultures (●) and in chloroform-treated cultures (○) at several time points over 60 minutes. The phage growth parameters are indicated in the figure and correspond to: E - eclipse period; L - latent period and B - burst size. Each data point is the mean of three independent experiments and error bars indicate the mean ± standard deviation.

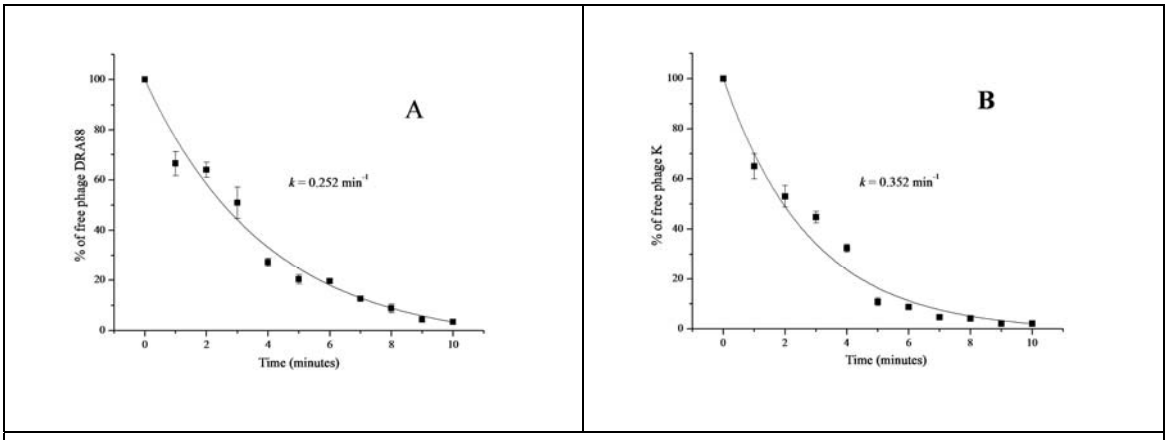

Figure 2: Percentage of free (A) DRA88 and (B) Phage K phages after infection of actively growing RN4220 *S. aureus* at a MOI of 0.001 at several time points over 10 minutes. Rate constants for loss of phage are 0.352 min^{-1} for Phage K and 0.252 min^{-1} for DRA88. Each data point is the mean of three independent experiments and error bars indicate the mean ± standard deviation.

789

790

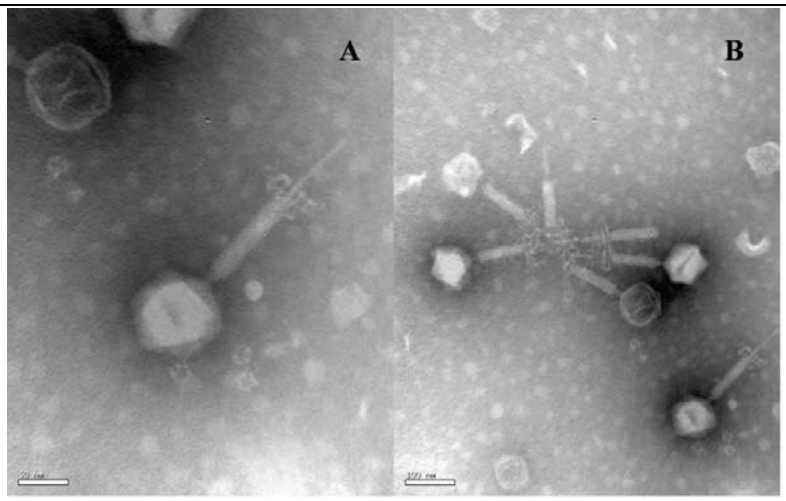

Figure 3: Electron micrograph images of phage DRA88 negatively stained with 1% uranyl acetate, (A) showing the tail in a contracted position and (B) formation on phage particles aggregates. Scale bar (50 nm (A) and 100 nm (B) is indicated.

791

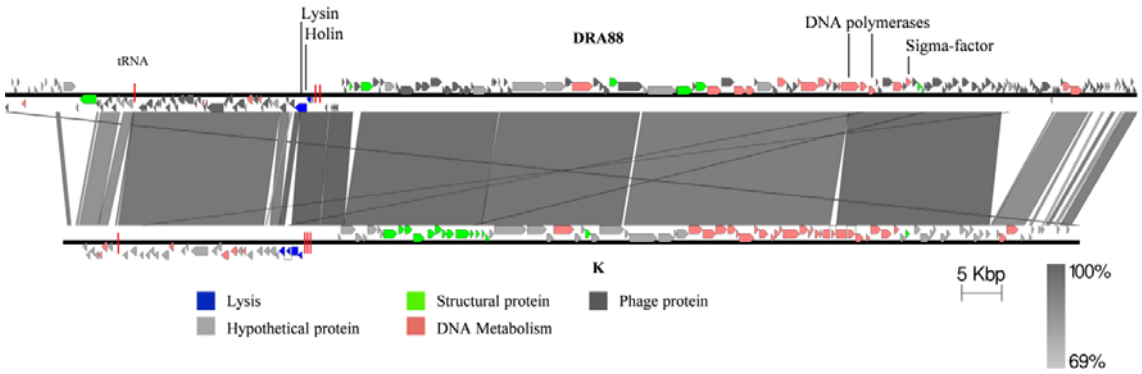

Figure 4: Comparative genomic analysis of phage DRA88 and phage K. Nucleotide sequences were compared using the Artemis Comparison Tool (ACT). Predicted ORFs are denoted by arrows, tRNAs are indicated (vertical blue dashed line) and genes encoding proteins with at least 69% amino acid identity between the two genomes are indicated by shaded regions.

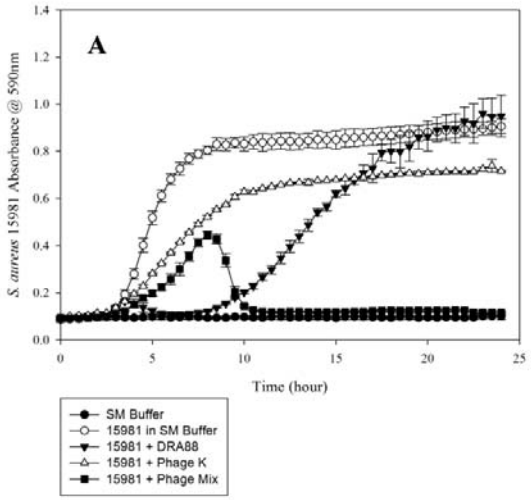

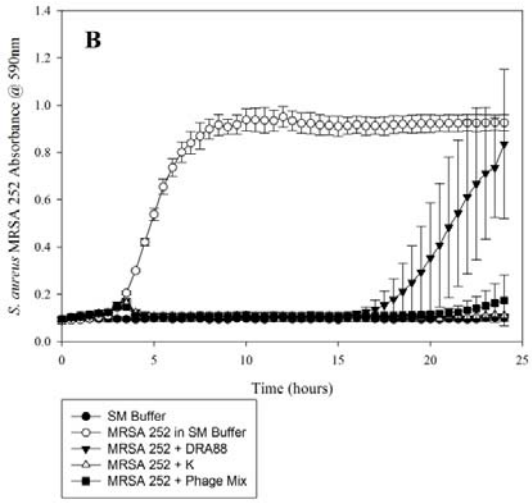

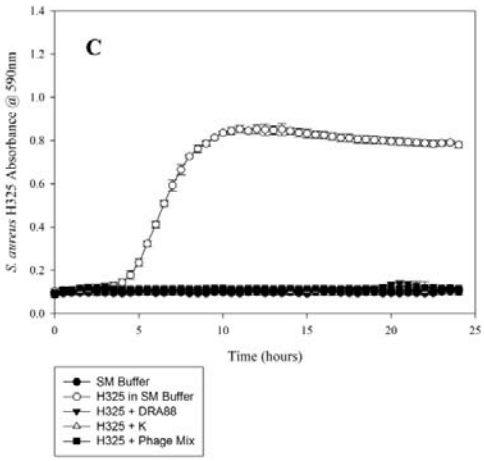

Figure 5: Dynamic of bacteria with single and phage mixture in liquid cultures over 24 hours incubation at 37 °C. Absorbance readings at 590nm were taken in a microtitre plate reader. *S. aureus* isolates: A – 15981; B – MRSA 252; C – H325 growing with only SM buffer (○), with single DRA88 (▼), with single phage K (△) and with the phage mixture in SM buffer (■) and also a negative control only SM buffer (●) are shown in the figure. Assays were performed four times and OD590 was expressed as the mean ± standard deviation.

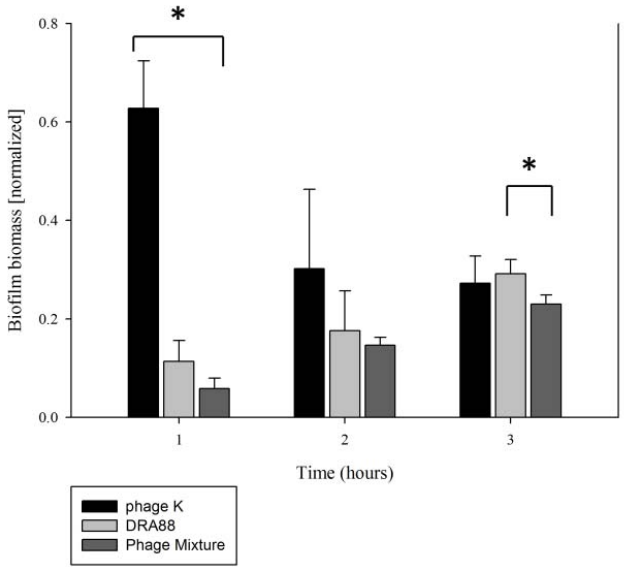

Figure 6 : Normalized biofilm biomass treated with single phage K, DRA88 and the phage mixture after 48 hours at MOI 10 (OD590 reading after CV staining). *S. aureus* isolates: 1 – 15981; 2 – MRSA 252; 3 – H325. Mean values for the three strains treated with: phage K = 0.63 (SD±0.10), 0.30 (SD±0.16), 0.27 (SD±0.06); DRA88 = 0.11 (SD±0.04), 0.18 (SD±0.08), 0.29 (SD±0.03) phage mixture = 0.06 (SD±0.02), 0.15 (SD±0.02), 0.23 (SD±0.02). Assays were performed three times and the mean ± standard deviation is indicated. Statistically significance of biofilm reduction was assessed by performing a *Student's t-test*. *p-values* are indicated (* : <0.05).

809

810

811

812

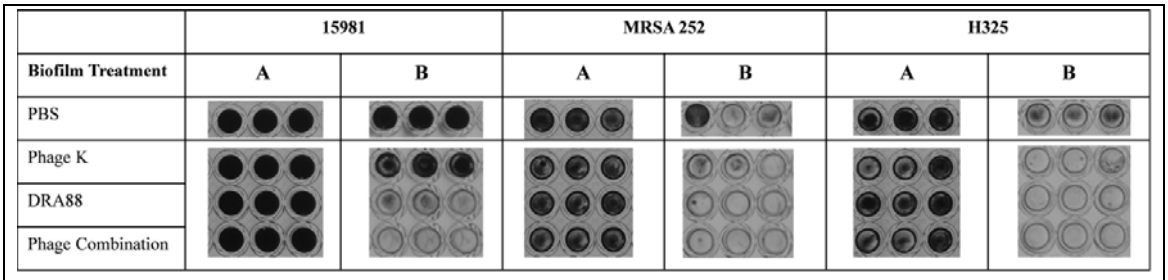

Figure 7: Visualization of wells stained with 0.1% of crystal violet after 48 hours of phage treatment at MOI 10. Shown are the biofilm wells treated with PBS, phage K, DRA88 and phage mixture at 0h (A) and (B) 48 hours after. Experiments were performed in triplicate.

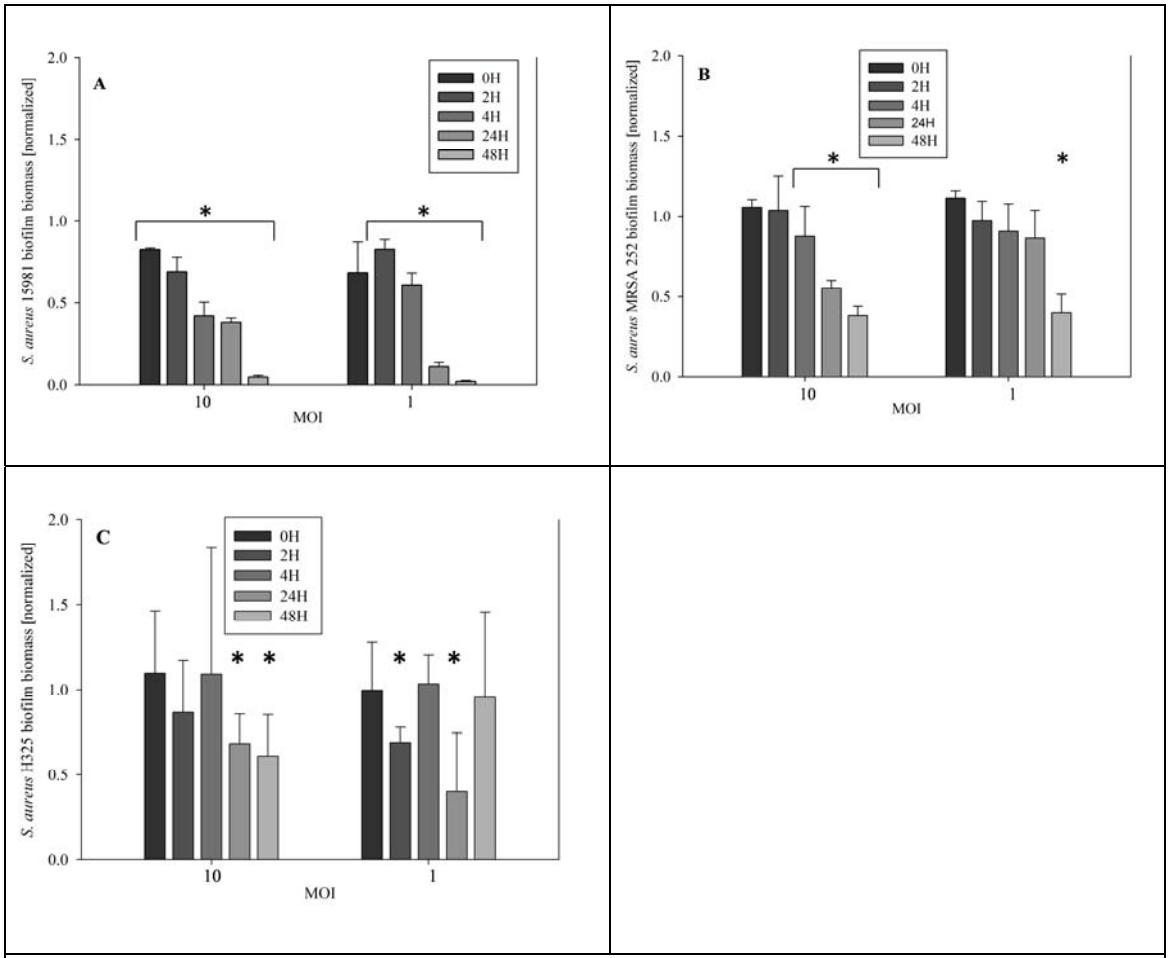

Figure 8: Normalized biofilm biomass treated with the phage mixture over 48 hours at two different MOIs (OD590 reading after CV staining). *S. aureus* isolates: A – 15981; B – MRSA 252; C – H325. Assays were performed three times and the mean ± standard deviation is indicated. Statistically significance of biofilm reduction was assessed by performing a *Student's t-test*. *p-values* are indicated (* : <0.05).

828

829